Temperature Estimation of Lithium-Ion Battery Based on an Improved Magnetic Nanoparticle Thermometer

DONGYAO ZOU[1], MING LI[1], DANDAN WANG[1], NANA LI[1], RIJIAN SU[1], PU ZHANG[2], YONG GAN[3], AND JINGJING CHENG [2]

[1]School of Computer and Communication Engineering, Zhengzhou University of Light Industry, Zhengzhou 450000, China
[2]School of Artificial Intelligence and Automation, Huazhong University of Science and Technology, Wuhan 430000, China
[3]Zhengzhou Institute of Technology, Zhengzhou 450000, China

Corresponding authors: Pu Zhang (puzhang08@hotmail.com) and Jingjing Cheng (chengjj2017@gmail.com)

ABSTRACT Lithium-ion batteries are widely used in new energy vehicles, especially electric vehicles. Temperature estimation is very important for battery life and safety. However, current temperature measurement methods cannot accurately measure the battery internal temperature. In this paper, a new method for battery temperature estimation based on an improved magnetic nanoparticle thermometer (MNPT) is proposed. The influence of dc magnetic field on temperature accuracy of a MNPT is firstly studied, the optimal dc magnetic field is found out under limitation of maximum temperature sensitivity and minimum temperature error, a new model of an improved MNPT is also established based on the ratio of first and second harmonics, and then the Lithium-ion battery temperature is estimated by use of the improved MNPT, the simulation and experiment results show that the improved MNPT can accurately estimate the battery internal temperature, which provides a new method for monitoring battery temperature of a new energy vehicle.

INDEX TERMS Lithium-ion battery, magnetic nanoparticle thermometer, new energy vehicle, battery temperature estimation.

I. INTRODUCTION

Due to high operating voltage, high power and energy density, long charge and discharge life, and no memory effect, lithium-ion batteries are widely used in electric vehicles [1]. However, a large amount of heat in the Lithium-ion battery packs will be accumulated during the charging and discharging process [2], [3]. The accumulated heat is difficult to spread out in time due to being limited in Lithium-ion battery structure, may seriously degrade the performance, decrease life-span of lithium-ion batteries, and lead to safety accident like spontaneous combustion [4]–[6]. It is very important to monitor accurately lithium-ion battery temperature of electric vehicles.

At present, the battery temperature measurement methods are shown in Table 1. The thermal resistor, thermocouple [7], [8] and infrared temperature measurement method [9], [10] can only measure the battery surface

temperature, cannot measure the internal temperature; the electrical impedance, and magnetic resonance [11]–[14] have a lower time resolution. Therefore, it is necessary to explore a new technology for accurately and quickly measuring the battery internal temperature.

Magnetic nanoparticles thermometer (MNPT) is a new, non-invasive method [15]–[23], which is based on magnetic nanoparticles (MNPs). Weaver *et al.* [15], Zhong *et al.* [17], Liu *et al.* [24] reported the temperature sensitivity of MNPs magnetization under an applied magnetic field. The magnetization of MNPs is nonlinear under an ac magnetic field, and MNPs temperature could be estimated by the ratio of the third and fifth harmonic. Li *et al.* [25], Zhong *et al.* [26], Yoshida and Enpuku [27] established theoretical model, and demonstrated that the fundamental f_0 and $2f_0$ harmonic amplitudes could be measured to calculate temperature when MNPs were exposed in ac and dc magnetic fields. Measurement error of fundamental f_0 and $2f_0$ harmonic amplitudes is considerably lower than that of $3f_0$ and $5f_0$ harmonics, because the harmonic amplitude is decreased rapidly with the

TABLE 1. Mainstream temperature measurement technology.

Method Type	Typical Sensor	Advantage	Weakness
Contact	Thermocouple / Thermal resistor	High precision, Fast speed	Unable to measure inside temp.
Radiation	Infrared Imager	Not contact, measure surface temp.	Unable to measure inside temp.
Electricity	Electrical Impedance	Not contact, measure inside temp.	Limited resolution, low accuracy
Magnetics	Magnetic Resonance	Not contact, measure temp. in depths	Complex influence factors, low limited solution

increased order of harmonics. Zhong *et al.* [28] investigated the influence of static magnetic field strength on the temperature sensitivity, and found that the temperature sensitivity of the ratio f_0 and $2f_0$ harmonics was significantly increased with increased dc magnetic field from 0.2 mT to 2.0 mT. However, it is a pity that they did not continue the studies in the case of higher dc magnetic field, and it is not clear whether the temperature sensitivity will further increase when the dc magnetic field exceeds 2.0 mT. The magnetization of MNPs, which is exposed to sufficiently large magnetic fields, will tend to saturate, and thus will no longer vary with temperatures. In other words, temperature sensitivity of MNPs, will decrease with increased dc magnetic field.

In this paper, we continue to study dc magnetic field dependence on temperature sensitivity and temperature error of a MNPT. The optimal range of the dc magnetic field strength (H_{dc}) is determined under the maximum temperature sensitivity and minimum temperature error of the MNPT. An improved magnetic nanometer thermometer is established, and employed to estimate Lithium-ion battery temperature.

II. THEORETICAL MODEL OF AN IMPROVED MAGNETIC NANOPARTICLES THERMOMETER FOR ESTIMATING LITHIUM-ION BATTERY TEMPERATURE

The ideal MNPs with a single core size and no interaction, the magnetization (M) of the MNPs under a magnetic field is described as follow:

$$M = NM_s[\coth(\frac{M_s VH}{kT}) - \frac{kT}{M_s VH}] \qquad (1)$$

where N is the number of MNPs per unit volume, M_s is saturation magnetization of a single MNP, V is volume of MNPs, k is Boltzmann constant, and T is absolute temperature, $H = H_{dc} + H_0 sin(2\pi f_0 \cdot t)$ is the applied magnetic field, H_0 is the amplitude of ac magnetic field, f_0 is the frequency of ac magnetic field, H_{dc} is the strength of dc magnetic field. The Equation (1) can be expanded by Taylor series. M_1 and M_2 are the amplitudes of fundamental f_0 and $2f_0$ harmonics of the MNP magnetization, respectively [29]–[32], which are expressed (2), as shown at the bottom of the next page.

Since other parameters are known, the ratio of the harmonic amplitudes of the fundamental f_0 and $2f_0$ harmonics is only related to the absolute temperature T. Therefore,

the problem of measuring battery temperature using MNPs is transformed into the inversion problem of amplitude detection of fundamental f_0 and $2f_0$ harmonics and temperature solution.

The f_0 and $2f_0$ harmonic amplitudes strongly depend on the dc magnetic field strength, the influence of different dc magnetic field strength on harmonic amplitudes is firstly simulated by use of MATLAB software on a PC. In simulations, the absolute temperature of magnetic nanoparticles was set at 314 K. The ac magnetic field has an amplitude of 1.0 mT and a frequency of 175 Hz. The strength of the dc magnetic field ranges from 0.01 mT to 300 mT with a step of 0.1 mT. The core diameter of the monodispersed MNPs is 30 nm and the saturation magnetization is 4.5×10^5 A/m. The sample frequency was set to 525 kHz, and the sample cycle was set to 9.

As shown in Fig. 1, M_1 declines sharply with H_{dc} increasing from 0.01 mT to 25 mT, then decreases slightly with H_{dc} increasing from 25 mT to 100 mT, and finally remains stable when H_{dc} exceeds 100 mT. It can be also seen that M_2 is considerable increased from 0.1 mT to 6.5 mT, and then is significantly decreased with H_{dc} from 6.5 mT to 25 mT, finally gradually stabilized as H_{dc} exceeds 100 mT.

It can be found that H_{dc} (0.01 mT to 25 mT) significantly affects M_1 and M_2. As H_{dc} exceeds 25 mT, the magnetization of the magnetic nanoparticle gradually becomes saturated and H_{dc} insignificantly affects M_1 and M_2. Therefore, there would be a maximal M_2 when H_{dc} ranges from 0.01 mT to 25 mT.

Although simulation reveals that H_{dc} between 0.01 mT and 25 mT significantly affects M_1 and M_2, the temperature sensitivity is an important factor for reducing the temperature error of a magnetic nanoparticle thermometer. The dependence of temperature sensitivity of M_1 and M_2 (dM_1/dT, dM_2/dT) on the strength of dc magnetic field is also needed to further study. The temperature sensitivities of the MNPs magnetization harmonics, such as dM_1/dT and dM_2/dT, are expressed (3), as shown at the bottom of the next page.

where dM_1/dT and dM_2/dT versus H_{dc} are depicted in Fig. 2. It can be found that the changing trends of dM_1/dT and dM_2/dT are similar to those of M_1 and M_2, respectively, with H_{dc} of 0.01 mT to 10 mT. That is, dM_1/dT and dM_2/dT are affected by H_{dc} from 0.01 mT to 10 mT. H_{dc} greater than 10mT insigni-ficantly affects the dM_1/dT and dM_2/dT. Consequently, simulation results show that H_{dc} from 0.01 mT
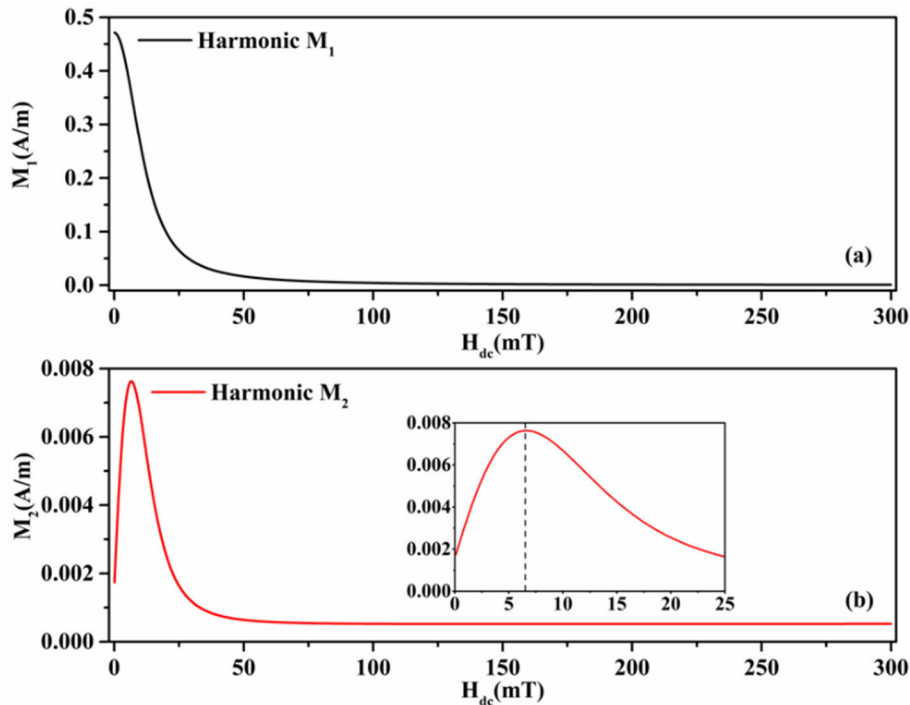
FIGURE 1. Simulated amplitudes of the fundamental f_0 and 2 f_0 harmonics (M_1, M_2) versus the strength of dc magnetic field (H_{dc}) at a temperature of 314K.

to 10 mT will influence on not only M_1 and M_2, but also dM_1/dT and dM_2/dT.

Eq. (3) shows that the temperature T could be calculated by employing the harmonic ratio M_2/M_1. Supposed that there are maximal M_2/M_1 and $d(M_2/M_1)/dT$ in the range of H_{dc}, the lowest temperature error of MNPT can be obtained. However, simulation results show that although maximal M_2 and dM_2/dT exist in H_{dc} of 0.01 mT to 10 mT, M_1 and dM_1/dT decreases with increasing H_{dc}. It is not also clear whether there is the optimal dc field range or not. So, the relationship between M_2/M_1, $d(M_2/M_1)/dT$, and H_{dc} is further studied. M_2/M_1 and $d(M_2/M_1)/dT$ versus H_{dc} are depicted in Fig. 3.

The ratio M_2/M_1 rises up gradually with H_{dc} increasing over the range 0.01 mT to 6 mT and then declines slightly

with H_{dc} increasing in the range of 6 mT to 10 mT, as shown in Fig. 3. It is not a great deal of difference between the changing trend of M_2/M_1 and $d(M_2/M_1)/dT$. The optimal range of H_{dc} is from 5.5 mT to 6.5 mT. M_2/M_1 and $d(M_2/M_1)/dT$ are optimal in the H_{dc} range of 5.5 mT to 6.5 mT. Consequently, the simulation result shows that the optimal H_{dc} ranges from 5.5 mT to 6.5 mT for the minimum temperature error of the MNPT.

III. EXPERIMENT AND RESULT

An improved MNPT, a temperature estimation system which includes PC controller part, excitation unit and detection unit was established, as shown in Fig. 4(a). NI-DAQ output ac + dc signal, amplified by a power amplifier, inputted the Helmholtz coils, and then generate ac and dc magnetic

$$\begin{cases} M_1 = NM_S \left[\frac{H_0}{3} \left(\frac{M_S V}{kT} \right) - \left(\frac{H_0^3}{60} + \frac{H_0 H_{dc}^2}{15} \right) \left(\frac{M_S V}{kT} \right)^3 + \left(\frac{H_0^5}{756} + \frac{H_0^3 H_{dc}^2}{63} + \frac{2H_0 H_{dc}^4}{189} \right) \left(\frac{M_S V}{kT} \right)^5 + \cdots \right] \\ M_2 = NM_S \left[\frac{H_0^2 H_{dc}}{30} \left(\frac{M_S V}{kT} \right)^3 - \left(\frac{H_0^4 H_{dc}}{189} + \frac{2H_0^2 H_{dc}^3}{189} \right) \left(\frac{M_S V}{kT} \right)^5 + \cdots \right] \end{cases} \quad (2)$$

$$\frac{dM_1}{dT} = NM_S \left[\begin{array}{l} -\frac{H_0}{3} \left(\frac{M_S V}{k} \right) \left(\frac{1}{T} \right)^2 + 3 \left(\frac{H_0^3}{60} + \frac{H_0 H_{dc}^2}{15} \right) \left(\frac{M_S V}{k} \right)^3 \left(\frac{1}{T} \right)^4 \\ -5 \left(\frac{H_0^5}{756} + \frac{H_0^3 H_{dc}^2}{63} + \frac{2H_0 H_{dc}^4}{189} \right) \left(\frac{M_S V}{k} \right)^5 \left(\frac{1}{T} \right)^6 + \cdots \end{array} \right]$$

$$\frac{dM_2}{dT} = NM_S \left[-3 \frac{H_0^2 H_{dc}}{30} \left(\frac{M_S V}{k} \right)^3 \left(\frac{1}{T} \right)^4 + 5 \left(\frac{H_0^4 H_{dc}}{189} + \frac{2H_0^2 H_{dc}^3}{189} \right) \left(\frac{M_S V}{k} \right)^5 \left(\frac{1}{T} \right)^6 + \cdots \right] \quad (3)$$
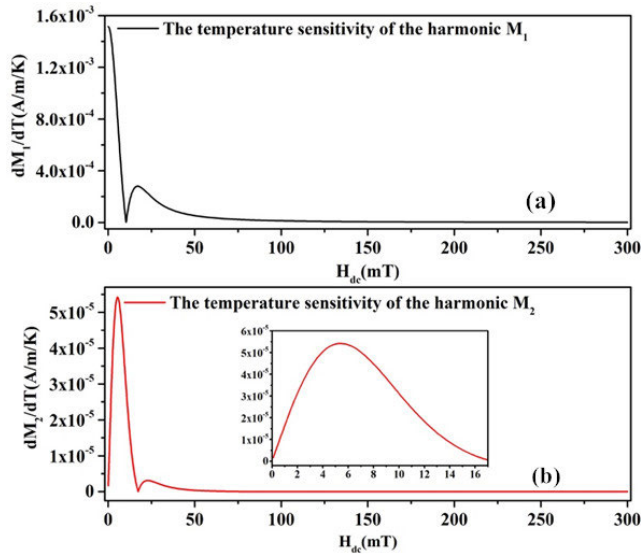
FIGURE 2. Simulated temperature sensitivity (dM_1/dT, dM_2/dT) versus the strength of dc magnetic field (H_{dc}) at a temperature of 314K.

FIGURE 3. Simulated harmonic ratio (M_2/M_1) and temperature sensitivity ($d(M_2/M_1)/dT$) versus the strength of dc magnetic field (H_{dc}) at a temperature of 314K.

fields. The detection unit converts the change in the magnetic field of the magnetic nanoparticles into a change in voltage through a detection coil, MNP magnetization is estimated by a pair of differential air-core coils, and then is amplified for pre-amplifier, which is detection unit. The system picture is shown in Fig. 4(b).

In the first experiment, the applied ac magnetic field was initially set at 1.0 mT and a frequency of 175 Hz. The dc magnetic field was set at 3.5 mT. Then, the magnetic nanoparticle samples were heated to 325 K in a water bath. Next, the samples were exposed to air for natural cooling in an air-conditioned room. Meanwhile, the sample temperature was estimated by Pt100. The amplitudes of the fundamental f_0 and $2f_0$ harmonics and harmonic ratios (M_2/M_1) vary with temperatures (310 K to 320 K). The temperature was calculated by Eq. (3). The temperature estimated by Pt100 was used as a benchmark for calculating the temperature error of the MNP thermometer. The experimental results are shown in Fig.5.
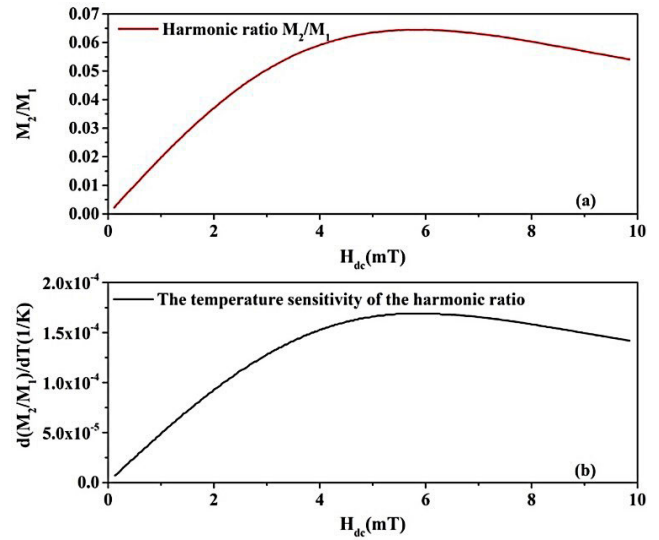
The temperature error between the magnetic nanoparticle thermometer and Pt100 is less than 0.15 K with the temperature of 310 K to 320 K. At this point, the harmonic measurement at a given H_{dc} were performed for 1 s. The experimental curves of the fundamental f_0 and $2f_0$ harmonics and the harmonic ratio (M_2/M_1) versus temperature are depicted in Fig. 6.

In the second experiment, we repeat the above experimental procedures at fixed temperature (314 K) and varied H_{dc} from 0.7 mT to 7.7 mT with a step of 1.4 mT. The experimental curves of M_2, M_1, and the ratio (M_2/M_1) at a temperature of 314 K under different H_{dc} are depicted in Fig.7. It can be found that the variation curves of M_2, M_1, and M_2/M_1 versus H_{dc} agree with those of the simulation results when H_{dc} ranges from 0.7 mT to 7.7 mT. There are maximum M_2 and M_2/M_1 at the dc magnetic field strength of 6.3 mT. The curve of $d(M_2/M_1)/dT$ at a temperature of 314 K under different H_{dc} is showed in Fig. 8. It can be found that
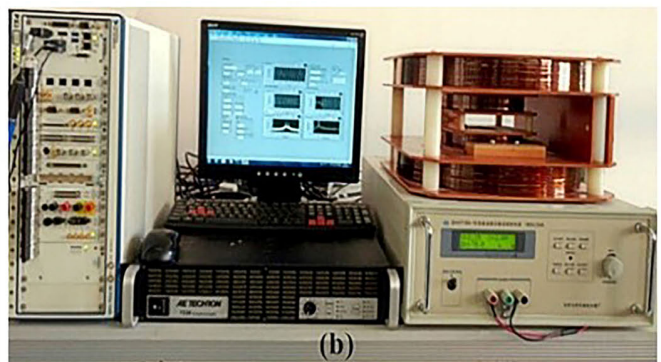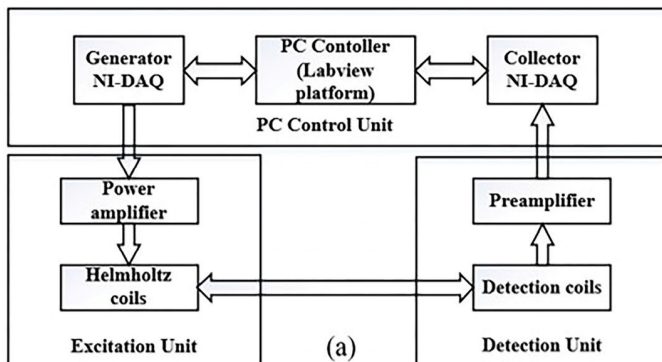

FIGURE 4. System of an improved magnetic nanoparticles thermometer, (a)System structure, (b) System picture.
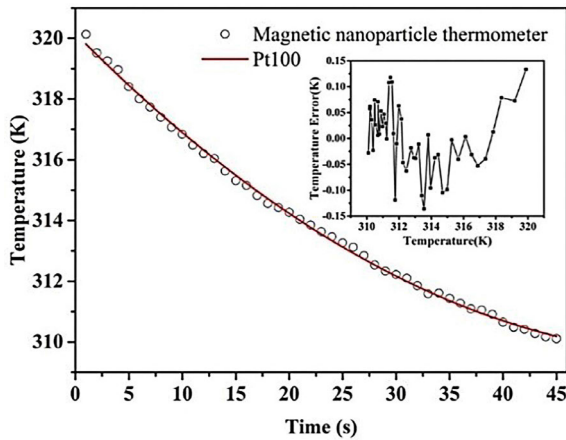
FIGURE 5. Comparison between the magnetic nanoparticle thermometer and Pt100 under different temperatures (310 K to 320 K).
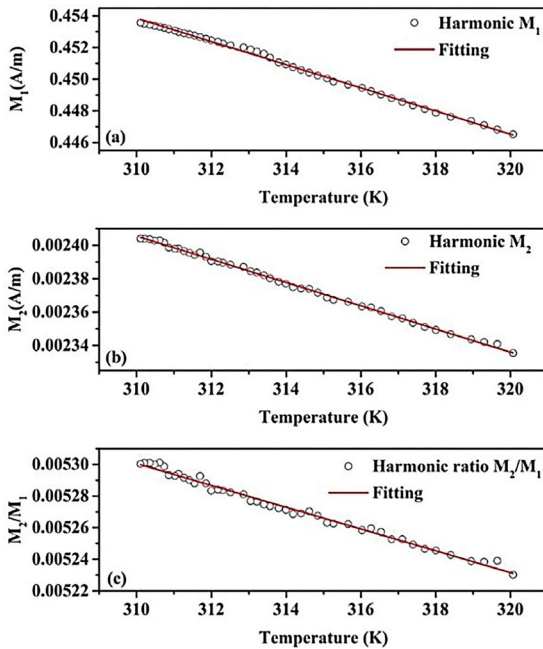

FIGURE 6. Experimental curves of the fundamental f_0 and $2f_0$ harmonics (M_1, M_2) and the ratio (M_2/M_1) versus temperature.

FIGURE 7. Experimental curves of the fundamental f_0 and $2f_0$ harmonics (M_2, M_1) and the ratio (M_2/M_1) versus the strength of the dc magnetic field (H_{dc}).

FIGURE 8. The $d(M_2/M_1)/dT$ versus dc magnetic field.

the variation in the curves of $d(M_2/M_1)/dT$ versus H_{dc} tally with those of the simulation results when H_{dc} ranges from 0.7 mT to 7.7 mT.

In the third experiment, the ac magnetic field was first set at 1.0 mT and a frequency of 175 Hz. H_{dc} was initially set at 0.7 mT. The Pt100 was inserted into the sample, and the magnetic nanoparticle samples were heated to 325 K in a water bath. Then, the samples were exposed to air for natural cooling in an air-conditioned room. Meanwhile, the sample temperature was measured by using a magnetic nanoparticle thermometer and a Pt100. Then, the temperature data were stored. Then, the standard temperature deviation of the magnetic nanoparticle thermometer (310 K to 320 K) with temperature measured by Pt100 is calculated as the benchmark.
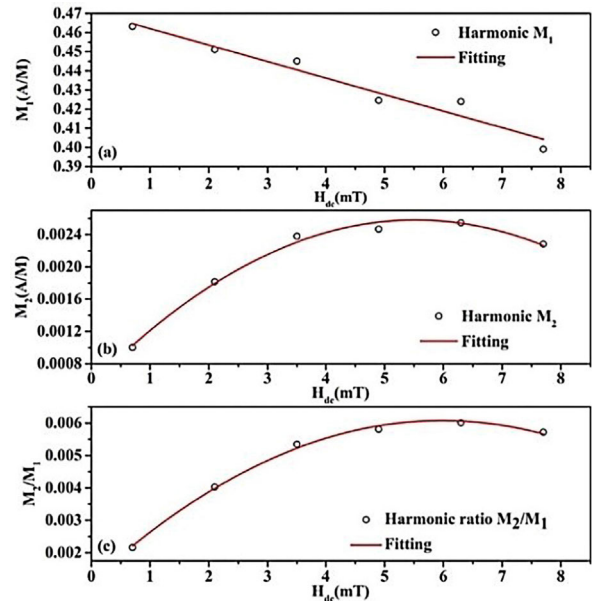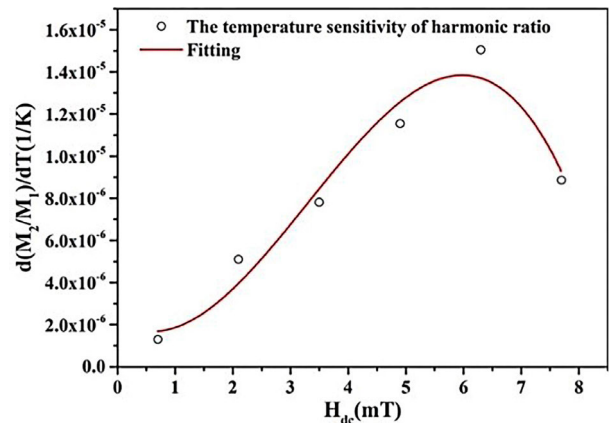
The experimental procedures were repeated under increasing H_{dc} from 0.7 mT to 7.7 mT with a step of 1.4 mT. The experimental results are shown in Fig.9. It can be found that the standard temperature deviation of the magnetic nanoparticle thermometer decreases as H_{dc} increases from 0.7 mT to 6.3 mT and then increases as H_{dc} exceeds 6.3 mT. Thus, the optimal H_{dc} which is between 6.0 mT and 6.5 mT, matches that of the simulation.

In the fourth experiment, we estimate Lithium-ion battery temperature by use of above improved MNPT. Lithium-ion battery is first prepared, and the internal structure of the battery pack used in the experiment is shown in figure 10. Since the battery temperature is mainly concentrated in the positive and negative electrode, during the battery production process, adhere the magnetic nanoparticles to the metal foil of the electrode through the thermal conductive silica gel. The
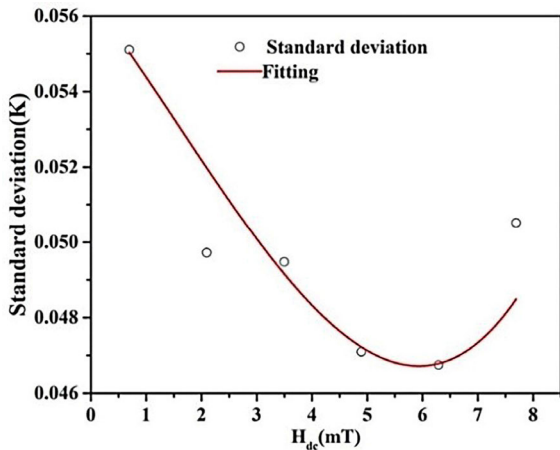
FIGURE 9. Comparison between the magnetic nanoparticle thermometer and Pt100 under different temperatures (310 K to 320 K).
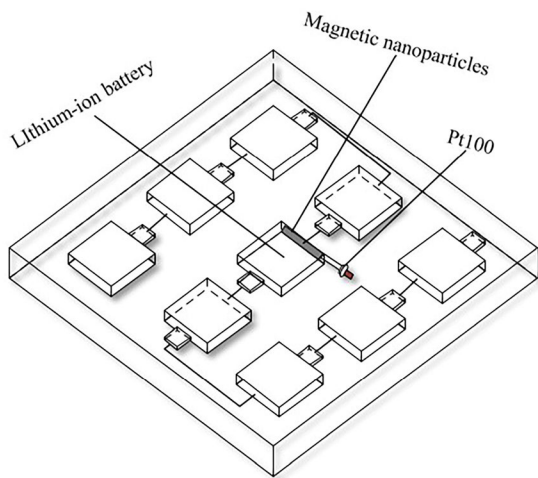

FIGURE 10. The internal structure of a layer of battery pack.

MNPs were directly coated on the negative electrode of the battery. A Pt100 was placed at the negative electrode of the battery sample for a comparative experiment. The experiment

results based on Pt100 can reflects the performance of an improved MNPT, such as temperature error, time resolution.

The reference ambient temperature of the battery charge and discharge test was set to 40 °C. First, charge the battery by the current of 2 C, after the battery was fully charged, the current was discharged by the current of 1 C, the temperature change of battery is shown in Fig.11(a). During the charging process, the battery temperature rises rapidly and the voltage will also rise rapidly with the increase of the current. When the battery is fully charged, the temperature rises slowly. When the discharge ends, the battery temperature reaches a maximum of 58.7 °C. It can be seen from the temperature curve of charge and discharge that the temperature change slightly lags behind the process of charging and discharging. When the discharge is completed, and the current is zero, the voltage also tends to be stable, the temperature of the battery reaches a maximum value. According to the experiment comparison between Pt100 and an improved MNPT, the temperature error of an improved MNPT is less than 0.5 i°C, is shown in figure 11 (b).

IV. CONCLUSION AND DISCUSSION

The mathematical model of battery temperature estimation is first established by using the harmonic amplitudes of the fundamental f_0 *and* $2f_0$ harmonics of the MNPs under a dc-ac magnetic field excitation system. The relationship between the fundamental f_0 and $2f_0$ harmonic amplitudes and their ratios to H_{dc} is studied. The optimal range of H_{dc} that provides maximum temperature sensitivity and minimum temperature error is determined. A temperature estimation system is established, and the experimental results are consistent with the simulation results. The temperature change curves in the process of Lithium-ion battery charging and discharging are estimated by an improved MNPT, and the temperature error is verified to be less than 0.5 °C by Pt100. An improved MNPT provides a new method for monitoring battery temperature of a new energy vehicle. However, the setup is a general-purpose system, which can estimate
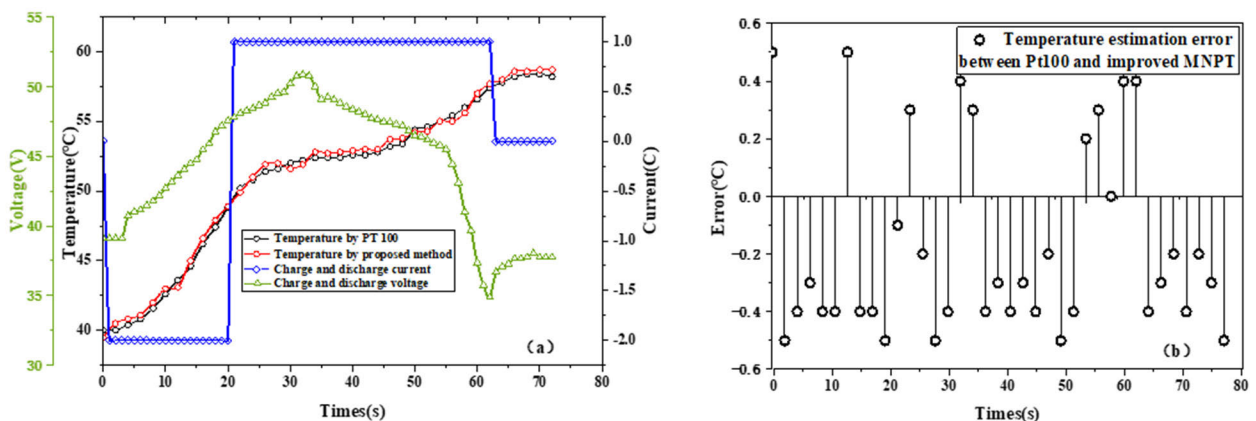

FIGURE 11. Battery temperature estimate system based on an improved magnetic nanoparticles thermometer, (a) Temperature change curve during the battery charging and discharging, (b) Temperature estimation error between Pt100 and improved magnetic nanoparticle thermometer.

the temperature of liquid/solid samples and PN junction of LED, the system is relatively bulky. In the next research, we will replace Helmholtz coils with Solenoid coil, reduce weight and size of system, and upgrade the system. The online experiments in the automobile will be carried out in the further research.

ACKNOWLEDGMENT

REFERENCES

[1] J. Jaguemont, L. Boulon, and Y. Dubé, "A comprehensive review of lithium-ion batteries used in hybrid and electric vehicles at cold temperatures," *Appl. Energy*, vol. 164, pp. 99–114, Feb. 2016.

[2] K. Fang, S. Chen, D. Mu, J. Liu, and W. Zhang, "The heat generation rate of nickel-metal hydride battery during charging/discharging," *J. Thermal Anal. Calorimetry*, vol. 112, no. 2, pp. 977–981, May 2013.

[3] J. P. Schmidt, S. Arnold, A. Loges, D. Werner, T. Wetzel, and E. Ivers-Tiffée, "Measurement of the internal cell temperature via impedance: Evaluation and application of a new method," *J. Power Sources*, vol. 243, pp. 110–117, Dec. 2013.

[4] R. Anderson, "Requirements for improved battery design and performance," *SAE Trans.*, vol. 99, pp. 1190–1197, Oct. 1990.

[5] S. J. Bazinski and X. Wang, "Experimental study on the influence of temperature and state-of-charge on the thermophysical properties of an LFP pouch cell," *J. Power Sources*, vol. 293, pp. 283–291, Oct. 2015.

[6] J. P. Schmidt, A. Weber, and E. Ivers-Tiffée, "A novel and precise measuring method for the entropy of lithium-ion cells: ΔS via electrothermal impedance spectroscopy," *Electrochimica Acta*, vol. 137, pp. 311–319, Aug. 2014.

[7] V. Blay and L. F. Bobadilla, "Numerical study of the accuracy of temperature measurement by thermocouples in small-scale reactors," *Chem. Eng. Res. Des.*, vol. 131, pp. 545–556, Mar. 2018.

[8] S. Panchal, R. Khasow, I. Dincer, M. Agelin-Chaab, R. Fraser, and M. Fowler, "Thermal design and simulation of mini-channel cold plate for water cooled large sized prismatic lithium-ion battery," *Appl. Thermal Eng.*, vol. 122, pp. 80–90, Jul. 2017.

[9] F. Song, C. Xu, S. Wang, and Z. Li, "Measurement of temperature gradient in a heated liquid cylinder using rainbow refractometry assisted with infrared thermometry," *Opt. Commun.*, vol. 380, pp. 179–185, Dec. 2016.

[10] D. Liu, G. Wang, Z. Nie, and Y. Rong, "An *in-situ* infrared temperature-measurement method with back focusing on surface for creep-feed grinding," *Measurement*, vol. 94, pp. 645–652, Dec. 2016.

[11] L. J. Anderson and M. V. Jacob, "Temperature dependent electrical impedance spectroscopy measurements of plasma enhanced chemical vapour deposited linalyl acetate thin films," *Thin Solid Films*, vol. 534, pp. 452–458, May 2013.

[12] J. Ilg, S. J. Rupitsch, and R. Lerch, "Temperature measurements by means of the electrical impedance of piezoceramics," in *Proc. IEEE Instrum. Meas. Technol. Conf.*, Oct. 2012, pp. 1851–1855.

[13] J. H. Hankiewicz, Z. Celinski, K. F. Stupic, N. R. Anderson, and R. E. Camley, "Ferromagnetic particles as magnetic resonance imaging temperature sensors," *Nature Commun.*, vol. 7, no. 1, Nov. 2016, Art. no. 12415.

[14] C. Ni and X. D. Zhou, "Method for reducing magnetic resonance temperature measurement errors in a magnetic resonance monitored HIFU treatment," U.S. Patent 8 638 099, Jan. 18, 2014.

[15] J. B. Weaver, A. M. Rauwerdink, C. R. Sullivan, and I. Baker, "Frequency distribution of the nanoparticle magnetization in the presence of a static as well as a harmonic magnetic field," *Med. Phys.*, vol. 35, no. 5, pp. 1988–1994, Apr. 2008.

[16] Z. Du , Y. Sun, J. Liu, R. Su, M. Yang, Y. Gan, and N. Ye, "Design of a temperature measurement and feedback control system based on an improved magnetic nanoparticle thermometer," *Meas. Sci. Technol.*, vol. 29, no. 4, 2018, Art. no. 045003.

[17] J. Zhong, W. Liu, L. Kong, and P. C. Morais, "A new approach for highly accurate, remote temperature probing using magnetic nanoparticles," *Sci. Rep.*, vol. 4, no. 1, May 2015, Art. no. 6338.

[18] Z. Du, "Key technology and application of magnetic nanometer temperature measurement," Ph.D. dissertation, Huazhong Univ. Sci. Technol., Wuhan, China, 2015.

[19] Z. Du, Y. Sun, R. Su, K. Wei, Y. Gan, N. Ye, C. Zou, and W. Liu, "The phosphor temperature measurement of white light-emitting diodes based on magnetic nanoparticle thermometer," *Rev. Sci. Instrum.*, vol. 89, no. 9, Sep. 2018, Art. no. 094901.

[20] Z. Du, R. Su, W. Liu, and Z. Huang, "Magnetic nanoparticle thermometer: An investigation of minimum error transmission path and AC bias error," *Sensors*, vol. 15, no. 4, pp. 8624–8641, Apr. 2015.

[21] Z. Du, Y. Sun, O. Higashi, Y. Noguchi, K. Enpuku, S. Draack, K.-J. Janssen, T. Kahmann, J. Zhong, T. Viereck, F. Ludwig, and T. Yoshida, "Effect of core size distribution on magnetic nanoparticle harmonics for thermometry," *Jpn. J. Appl. Phys.*, vol. 59, no. 1, Jan. 2020, Art. no. 010904.

[22] A. M. Rauwerdink and J. B. Weaver, "Viscous effects on nanoparticle magnetization harmonics," *J. Magn. Magn. Mater.*, vol. 322, no. 6, pp. 609–613, Mar. 2010.

[23] J. B. Weaver, A. M. Rauwerdink, and E. W. Hansen, "Magnetic nanoparticle temperature estimation," *Med. Phys.*, vol. 36, no. 5, pp. 1822–1829, Apr. 2009.

[24] W. Liu, J. Zhong, Q. Xiang, G. Yang, and M. Zhou, "Discretization of magnetization curves and their application in size estimation of nanosized ferrofluid," *IEEE Trans. Nanotechnol.*, vol. 10, no. 6, pp. 1231–1237, Nov. 2011.

[25] W. Liu and J. Zhong, "Comparison of noninvasive and remote temperature estimation employing magnetic nanoparticles in DC and AC applied fields," in *Proc. IEEE Int. Instrum. Meas. Technol. Conf.*, May 2012, pp. 2738–2741.

[26] J. Zhong, J. Dieckhoff, M. Schilling, and F. Ludwig, "Influence of static magnetic field strength on the temperature resolution of a magnetic nanoparticle thermometer," *J. Appl. Phys.*, vol. 120, no. 14, Oct. 2016, Art. no. 143902.

[27] T. Yoshida and K. Enpuku, "Simulation and quantitative clarification of AC susceptibility of magnetic fluid in nonlinear brownian relaxation region," *Jpn. J. Appl. Phys.*, vol. 48, no. 12, Dec. 2009, Art. no. 127002.

[28] J. Zhong, W. Liu, Z. Du, P. César de Morais, Q. Xiang, and Q. Xie, "A noninvasive, remote and precise method for temperature and concentration estimation using magnetic nanoparticles," *Nanotechnology*, vol. 23, no. 7, Feb. 2012, Art. no. 075703.

[29] Z. Du, Y. Sun, O. Higashi, K. Enpuku, and T. Yoshida, "Empirical expression for harmonics of AC magnetization of magnetic nanoparticles with core size distribution," *Jpn. J. Appl. Phys.*, vol. 58, no. 9, Sep. 2019, Art. no. 097003.

[30] J. Zhong, W. Liu, M. Zhou, and L. He, "AC magnetization measurement employing a pair of differentiating coils for magnetic nanoparticle noninvasive and remote temperature estimation," in *Proc. IEEE Int. Instrum. Meas. Technol. Conf. Proc.*, May 2012, pp. 1780–1783.

[31] I. M. Perreard, D. B. Reeves, X. Zhang, E. Kuehlert, E. R. Forauer, and J. B. Weaver, "Temperature of the magnetic nanoparticle microenvironment: Estimation from relaxation times," *Phys. Med. Biol.*, vol. 59, no. 5, pp. 1109–1119, Mar. 2014.

[32] E. Garaio, J.-M. Collantes, J. A. Garcia, F. Plazaola, and O. Sandre, "Harmonic phases of the nanoparticle magnetization: An intrinsic temperature probe," *Appl. Phys. Lett.*, vol. 107, no. 12, Sep. 2015, Art. no. 123103.

DONGYAO ZOU received the B.S. degree in industrial automation from Zhengzhou University, in 1996, and the M.S. degree in microelectronics and solid-state electronics and the Ph.D. degree in circuits and systems from the Beijing University of Posts and Telecommunications, in 2005 and 2008, respectively. Since July 2008, he has been engaged in teaching and research work with the School of Computer and Communication Engineering, Zhengzhou University of Light Industry. His research interests include design of magnetometer and susceptometer and applications in nano-magnetic measurement.

MING LI received the B.S. degree in the Internet of Things engineering from the School of Computer and Communication Engineering, Zhengzhou University of Light Industry, Zhengzhou, China, where she is currently pursuing the M.S. degree in signal and information processing. Her research interest includes magnetic nano-meter thermometers for applications in biomedical and industrial field.

DANDAN WANG received the B.S. degree in electronic information science and technology from the School of Computer and Communication Engineering, Zhengzhou University of Light Industry, Zhengzhou, China, where she is currently pursuing the M.S. degree in computer science and technology. Her research interest includes magnetic nano-meter thermometers for applications in biomedical and industrial field.

NANA LI received the M.S. degree in communication and information system from the Beijing University of Posts and Telecommunications, in 2006. She is currently an Associate Professor with the School of Computer and Communication Engineering, Zhengzhou University of Light Industry, Zhengzhou, China. Her research interests include design of magnetometer and susceptometer and applications in nano-magnetic measurement.

RIJIAN SU received the Ph.D. degree in control science and engineering from the Huazhong University of Science and Technology, in 2010. He is currently a Professor with the School of Computer and Communication Engineering, Zhengzhou University of Light Industry, Zhengzhou, China. His research interests include detection and control, embedded systems, and intelligent computing based on magnetic nanoparticles temperature measurement information processing technology research.

PU ZHANG received the B.S. degree in detection technology and automation instrumentation and the M.S. degree in control science and engineering from the Huazhong University of Science and Technology, in 1988 and 2002, respectively. She is currently an Associate Professor with the School of Automation, Huazhong University of Science and Technology. Her research interests include sensing technology, measurement and control systems, and magnetic nano-meter thermometers for applications in biomedical and industrial field.

YONG GAN received the B.S. degree from Xi'an Jiaotong University, in 1986, and the M.S. degree from the Space Department, Shaanxi Institute of Microelectronics, in 1989. He is currently a Vice President with the School of Zhengzhou Institute of Technology. His main research interests include computer network and its application and magnetic nano-meter thermometers for applications in biomedical and industrial field.

JINGJING CHENG received the B.S. degree in automation, the M.S. degree in detection technology and automation equipment, and the Ph.D. degree in control science and engineering from the Huazhong University of Science and Technology, in 1999, 2002, and 2011, respectively. His main research interests include information theory and its acquisition method, low-field nuclear magnetic resonance measurement technology, deep-sea exploration technology, and magnetic nano-meter thermometers for applications in biomedical and industrial field.

$\bullet\ \bullet\ \bullet$